Functional Importance of Second Heart Field-derived Cells During Thoracic Aortic Aneurysm Formation

Hisashi Sawada[1], Hideyuki Higashi[3], Debra L. Rateri[1], Jeff Z. Chen[1, 2], Jessica J. Moorleghen[1], Deborah A. Howatt[1], Hong S. Lu[1, 2], Stephanie Morgan[3], Sasha A. Singh[3], Masanori Aikawa[3], Mark W. Majesky[4], Alan Daugherty[1,2]

1. Saha Cardiovascular Research Center, University of Kentucky, KY
2. Department of Physiology, University of Kentucky, KY
3. Center for Interdisciplinary Cardiovascular Sciences, Cardiovascular Division, Department of Medicine, Brigham and Women's Hospital, Harvard Medical School, Boston, MA
4. Center for Developmental Biology & Regenerative Medicine, Seattle Children's Research Institute, Departments of Pediatrics and Pathology, University of Washington, Seattle, WA

Running Title: SHF-derived cells impact TAA

Corresponding Author:
Alan Daugherty
Saha Cardiovascular Research Center, University of Kentucky
741 South Limestone Street
BBSRB, B243
Lexington, KY, 40536
Tel: +1-859-323-3512
E-mail: alan.daugherty@uky.edu

Keywords: embryonic origin, smooth muscle cells, second heart field, ascending aorta, thoracic aortic aneurysm, Lrp1, TGF-β

Word count:
Abstract: 64 words
Manuscript: 1500 words

Abstract
Embryonic origins of smooth muscle cells (SMCs) may contribute to regional specificity of thoracic aortic aneurysms. Here, we demonstrate that SMCs derived from the second heart field localized with angiotensin II-induced aortopathies. Proteomics analysis discerned potential roles of Lrp1 and TGF-β pathways, and genetic ablation of these pathways in second heart field-derived cells augmented aortopathies, indicating functional importance of this origin on aortic integrity.

Thoracic aortic aneurysms (TAAs), commonly occurring in the ascending aorta,[1,2] exhibit a medial gradient disruption with outer layers most greatly affected.[3-8] Smooth muscle cells (SMCs), a major component of the media, in this region are derived from two embryonic origins: cardiac neural crest (CNC) and second heart field (SHF).[9] While grossly indistinguishable, lineage tracking studies have demonstrated that CNC-and SHF-derived SMCs occupy inner and outer layers, respectively.[10] Although regional distribution of SHF-derived SMCs coincides with TAA location, the role of SHF origin in aortic wall integrity is unclear. In this study, we addressed the functional importance of SHF origin on regional specificity and development of TAAs.

Mass spectrometry-assisted proteomics investigated mechanisms driving regional specificity of TAAs. Using angiotensin II (AngII) infusion to induce TAAs,[11] aortic tissues were harvested just prior to overt pathology. Negative controls included saline infusion and aneurysm resistant descending aorta. Proteomics analysis identified 2644 proteins. In principal component analyses using the unfiltered proteome, protein profiles of ascending and descending aortas in saline-infused mice were not significantly different. However, AngII infusion altered these profiles significantly compared to saline and region **(**40% variation along PC1, **Fig 1a)**. In the ascending aorta, AngII infusion changed 864 protein abundances compared to saline-infused group **(Fig 1b)**. Within AngII-infused mice, abundances of 77 proteins were different between ascending and descending aortas **(Fig 1b)**. Forty two proteins were common between these two subsets, indicating that these molecules may be a specific target for TAA formation **(Fig 1b, c)**. Accumulating literature indicates that LDL receptor-related protein 1 (Lrp1), a multi-functional protein expressed in SMCs, contributes to aortic wall integrity.[12-14] Thus, protein-protein interaction of Lrp1 and 42 overlapped molecules were investigated. Lrp1 interacted with 10 proteins including several Lrp1 ligands: serpine1, thrombospondin1, and matrix metalloproteinase2, and AngII altered abundance of these molecules **(Fig 1d, e)**. We next examined interactions between SMC origin and AngII-induced aortic pathology. CNC- and SHF-derived cells were tracked using Wnt1-*Cre* or Mef2c-*Cre* ROSA26R^{LacZ} mice infused with AngII. Consistent with our previous study, the ascending aorta was composed of both CNC- and SHF-derived SMCs with neither extending beyond the aortic arch **(Fig 1f)**. AngII infusion did not alter their distribution, whereas medial thickening occurred in outer layers where SMCs derive from the SHF **(Fig 1g)**. Altogether, these data suggest that Lrp1 in SHF-derived SMCs exerts a critical role in AngII-induced aortic pathologies.

Deletion of *Lrp1* in SMCs causes multiple aortic pathologies,[12-14] but it was unclear whether its deletion in a specific SMC origin affects TAA formation. Therefore, we deleted Lrp1 in either CNC or SHF-derived SMCs. CNC-specific deletion of *Lrp1* using the Wnt1 promoter to drive *Cre* expression was embryonically lethal between E11.5 and E12.5 **(Supplementary Fig 1a)**. Gross appearance was comparable between genotypes at E11.5 with no obvious vascular malformation **(Supplementary Fig 1b)**. Since this promoter is not restricted to the aorta **(Supplementary Fig 2)**, extra-aortic *Lrp1* deletion may have contributed to embryonic lethality. Next, *Lrp1* was deleted in SHF-derived SMCs using a Mef2c promoter driven *Cre*. SHF-specific *Lrp1* deletion did not affect growth or development of the mice and restricted to outer medial layers. Lrp1 abundance was reduced by 37% in the ascending aortic media of *Cre*-expressing

mice compared to wild type littermates **(Supplementary Fig 3a-f)**. To promote TAAs, AngII was infused for 4 weeks resulting in significant augmentation of aortic dilation and exacerbated ascending aortic rupture and elastin fragmentation by *Lrp1* deletion in SHF-derived cells **(Fig 2a-e)**. Systolic blood pressure was not different between genotypes in response to AngII infusion **(Fig 2f)**, demonstrating augmented aortopathy was independent of blood pressure. Aortic pathologies were not observed in the descending aorta of either genotype **(Fig 2a)**. To explore molecular mechanisms behind Lrp1 augmented TAAs, proteomics analysis was performed using aortas harvested from wild type and SHF-specific *Lrp1* deleted mice prior to overt pathology. Deletion of *Lrp1* in the ascending aorta of Mef2c-*Cre* +/0 mice was confirmed **(Supplementary Fig 4)**. Based on $q < 0.1$ threshold, deletion of *Lrp1* in SHF-derived cells altered abundances of seven proteins with six of them linked to transforming growth factor β (TGF-β) signaling molecules **(Fig 2g, h)**. These results indicated that the protective function of *Lrp1* in SHF-derived SMCs against AngII-induced TAA associates with alteration of TGF-β signaling-related proteins.

Genetic mutations of TGF-β type 2 receptor (Tgfbr2) cause Loeys-Dietz syndrome (LDS) with probands predisposed to aneurysms.[15] In mice, postnatal deletion of *Tgfbr2* in SMCs promotes severe TAA formation with pathologies localized to outer medial layers of the ascending aorta.[5,16] Since regional and transmural location of pathologies in LDS corresponded to distribution of SHF-derived SMCs, we investigated the role of Tgfbr2 in SHF-derived cells on aortic structure. SHF-specific *Tgfbr2*-depletion was embryonic lethal beginning at E12.5 **(Fig 2i)**. The outflow tract was significantly dilated in fetuses with SHF-specfic Tgfbr2 deletion compared to wild type littermates **(Fig 2i)**. These data, alongside our findings in SHF-derived Lrp1, indicate that SHF-derived SMCs play a critical role in aortic structure and ascending aneurysm development.

Our study demonstrates the functional importance of SHF-derived cells in ascending aortic wall integrity using multiple TAA mouse models. In contrast to our findings, recent studies in the aortic root provided conflicting results on contribution of CNC- and SHF-derived cells to aortic dilation.[17,18] It is possible that these two developmental origins have divergent pathophysiological functions in different aortic regions. Thus, heterogeneity of SMC origins contributes to complex mechanisms of aneurysm formation, which should be considered when investigating TAA pathophysiology.

Methods

Methods, including statements of data availability and any associated accession codes and references, are available in the online version of the paper.

Acknowledgments

The authors' research work was supported by the National Heart, Lung, and Blood Institute of the National Institutes of Health under award numbers [R01HL133723 (AD), R01HL126901 (MA), R01HL149302 (MA), R01HL121877 (MWM)] and the American Heart Association SFRN in Vascular Disease (18SFRN33960001). HS was supported by an AHA postdoctoral fellowship (18POST33990468). JC was supported by NCATS

UL1TR001998 and NHLBI F30HL143943. The content in this manuscript is solely the responsibility of the authors and does not necessarily represent the official views of the National Institutes of Health.

Competing Financial Interests

The following authors do not have conflict to declare: HS, DLR, JZC, JJM, DAH, HSL, SAS, MA, MWM, AD. HH is an employee of Kowa Company, Ltd. (Nagoya, Japan) and was a visiting scientist at Brigham and Women's Hospital when the study was conducted.

Figure Legends

Figure 1.

(a) Principal component analysis of the unfiltered proteome. Asc = ascending aorta, Desc = descending aorta (n = 3 – 4). **(b)** Venn diagram of differentiated proteins ($q < 0.1$). **(c)** Heat map with Z score coloring for overlapped 42 proteins. **(d)** Protein-protein interaction between overlapped 42 proteins and Lrp1. **(e)** Fold change of protein intensity related to Lrp1 in overlapped 42 proteins compared to AngII- and saline-infused ascending aortas. **(f)** Representative images of X-gal stained aortas and hearts from Wnt1- and Mef2c-*Cre* ROSA26R^{LacZ} mice (n = 3). IA = innominate artery, LCA = left common carotid artery, LSA = left subclavian artery. **(g)** Representative X-gal staining and FITC images of aortas from saline or AngII-infused Wnt1- and Mef2c-*Cre* ROSA26R^{LacZ} mice (n = 5 – 7). Yellow triangles indicate medial thickening. Scale bar = 50 µm.

Figure 2.

(a) Representative ultrasound images and gross appearances of ascending aortas. Asc = ascending aorta, IA = innominate artery. Scale bar = 1 mm. **(b)** Ascending aortic diameter measured by ultrasonography. *** = $p < 0.001$. **(c)** Survival rate from ascending aortic rupture. n = 21 – 40. **(d)** Representative Movat's and Verhoeff iron hematoxylin staining. Scale bar = 50 µm. **(e)** Elastin break counts in Movat's stained sections. **(f)** Systolic blood pressure. **(g)** Heat map with Z score coloring for differentiated proteins in comparison between wild type and SHF-specific *Lrp1* deleted ascending aortas ($q < 0.1$, n = 3 – 5). **(h)** Protein-protein interaction between 7 identified proteins and TGF-β signaling molecules. Red font indicates proteins related to TGF-β signaling. **(i)** Representative images of gross appearance and outflow tract of dead (middle) and survived (right) fetuses with SHF-specific *Tgfbr2* deletion and wild type littermates (left) at E12.5. Blue dotted lines indicate the edge of the outflow tract. **(j)** Outflow diameter was measured at 300 – 400 µm distal of the root of fetuses that survived at the termination. n = 5 – 7. Scale bar = 1 mm.

References

1. Isselbacher, E.M. *Circulation* **111**, 816-828 (2005).
2. Albornoz, G.*, et al. Ann Thorac Surg* **82**, 1400-1405 (2006).
3. Trachet, B.*, et al. Arterioscler Thromb Vasc Biol* **36**, 673-681 (2016).
4. Daugherty, A.*, et al. Clin Sci (Lond)* **118**, 681-689 (2010).
5. Li, W.*, et al. J Clin Invest* **124**, 755-767 (2014).
6. Wanga, S.*, et al. J Pathol* **243**, 294-306 (2017).
7. Sawada, H.*, et al. J Transl Int Med* **6**, 93-96 (2018).
8. Yang, P.*, et al. Sci Rep* **6**, 35444 (2016).
9. Majesky, M.W. *Arterioscler Thromb Vasc Biol* **27**, 1248-1258 (2007).
10. Sawada, H., Rateri, D.L., Moorleghen, J.J., Majesky, M.W. & Daugherty, A. *Arterioscler Thromb Vasc Biol* **37**, 1722-1726 (2017).
11. Rateri, D.L.*, et al. Am J Pathol* **184**, 2586-2595 (2014).
12. Basford, J.E.*, et al. PLoS One* **8**, e82026 (2013).
13. Boucher, P., Gotthardt, M., Li, W.P., Anderson, R.G. & Herz, J. *Science* **300**, 329-332 (2003).
14. Davis, F.M.*, et al. Arterioscler Thromb Vasc Biol* **35**, 155-162 (2015).
15. Lindsay, M.E. & Dietz, H.C. *Nature* **473**, 308-316 (2011).
16. Hu, J.H.*, et al. Arterioscler Thromb Vasc Biol* **35**, 2647-2656 (2015).
17. Koenig, S.N.*, et al. JCI Insight* **2**(2017).
18. MacFarlane, E.G.*, et al. J Clin Invest* **129**, 659-675 (2019).

Figure 1.

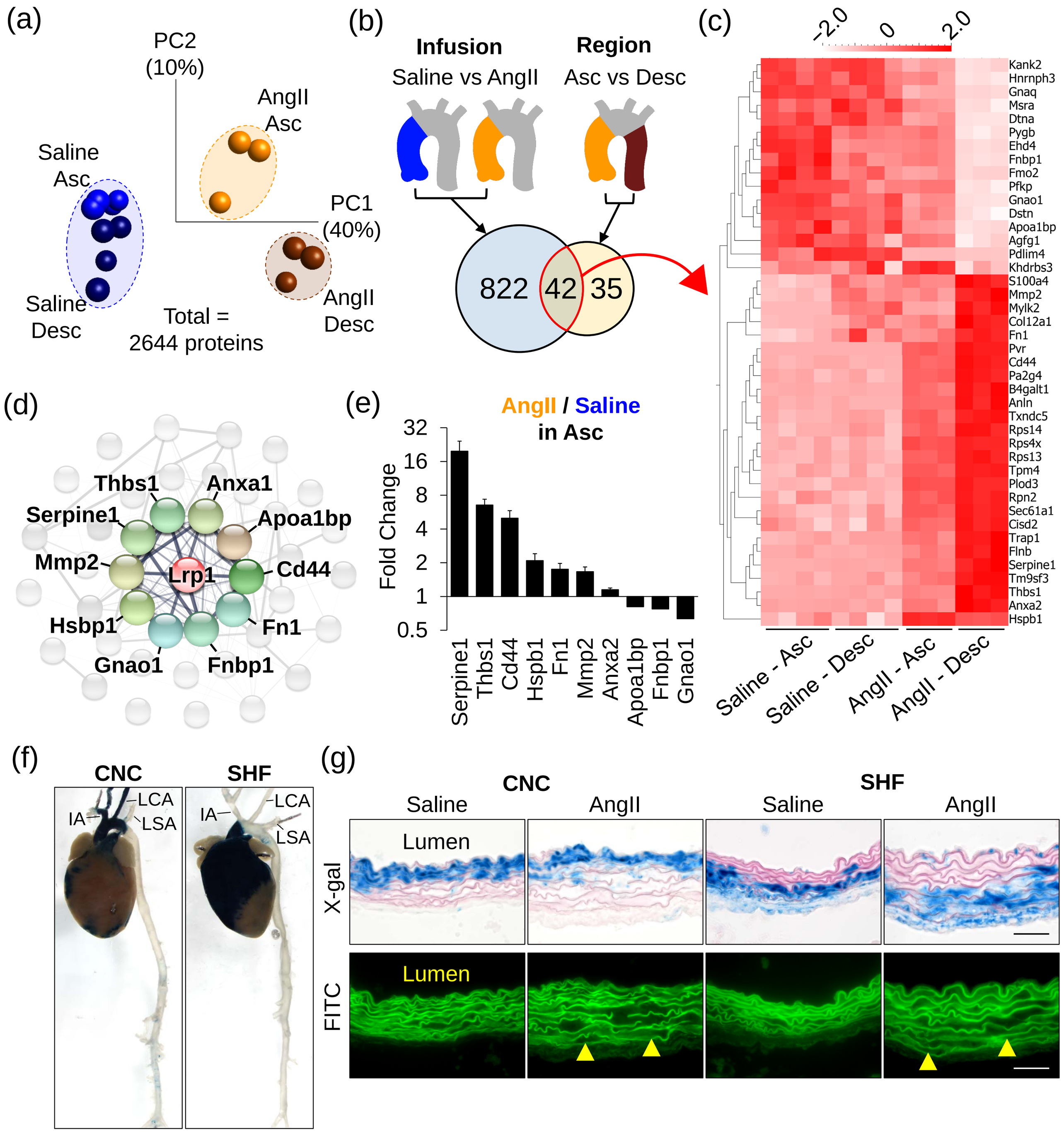
(a)
PC2
(10%)
AngII
Asc
Saline
Asc
PC1
(40%)
Saline
Desc
AngII
Desc
Total =
2644 proteins
(b)
Infusion
Saline vs AngII
Region
Asc vs Desc
822
42
35
(c)
-2.0
0
2.0
Kank2
Hnrnph3
Gnaq
Msra
Dtna
Pygb
Ehd4
Fnbp1
Fmo2
Pfkp
Gnao1
Dstn
Apoa1bp
Agfg1
Pdlim4
Khdrbs3
S100a4
Mmp2
Mylk2
Col12a1
Fn1
Pvr
Cd44
Pa2g4
B4galt1
Anln
Txndc5
Rps14
Rps4x
Rps13
Tpm4
Plod3
Rpn2
Sec61a1
Cisd2
Trap1
Flnb
Serpine1
Tm9sf3
Thbs1
Anxa2
Hspb1
Saline - Asc
Saline - Desc
AngII - Asc
AngII - Desc
(d)
Thbs1
Anxa1
Serpine1
Apoa1bp
Mmp2
Lrp1
Cd44
Hsbp1
Fn1
Gnao1
Fnbp1
(e)
AngII / Saline
in Asc
Fold Change
32
16
8
4
2
1
0.5
Serpine1
Thbs1
Cd44
Hspb1
Fn1
Mmp2
Anxa2
Apoa1bp
Fnbp1
Gnao1
(f)
CNC
SHF
IA
LCA
LSA
(g)
CNC
SHF
Saline
AngII
Saline
AngII
X-gal
FITC
Lumen
Lumen

Figure 2.

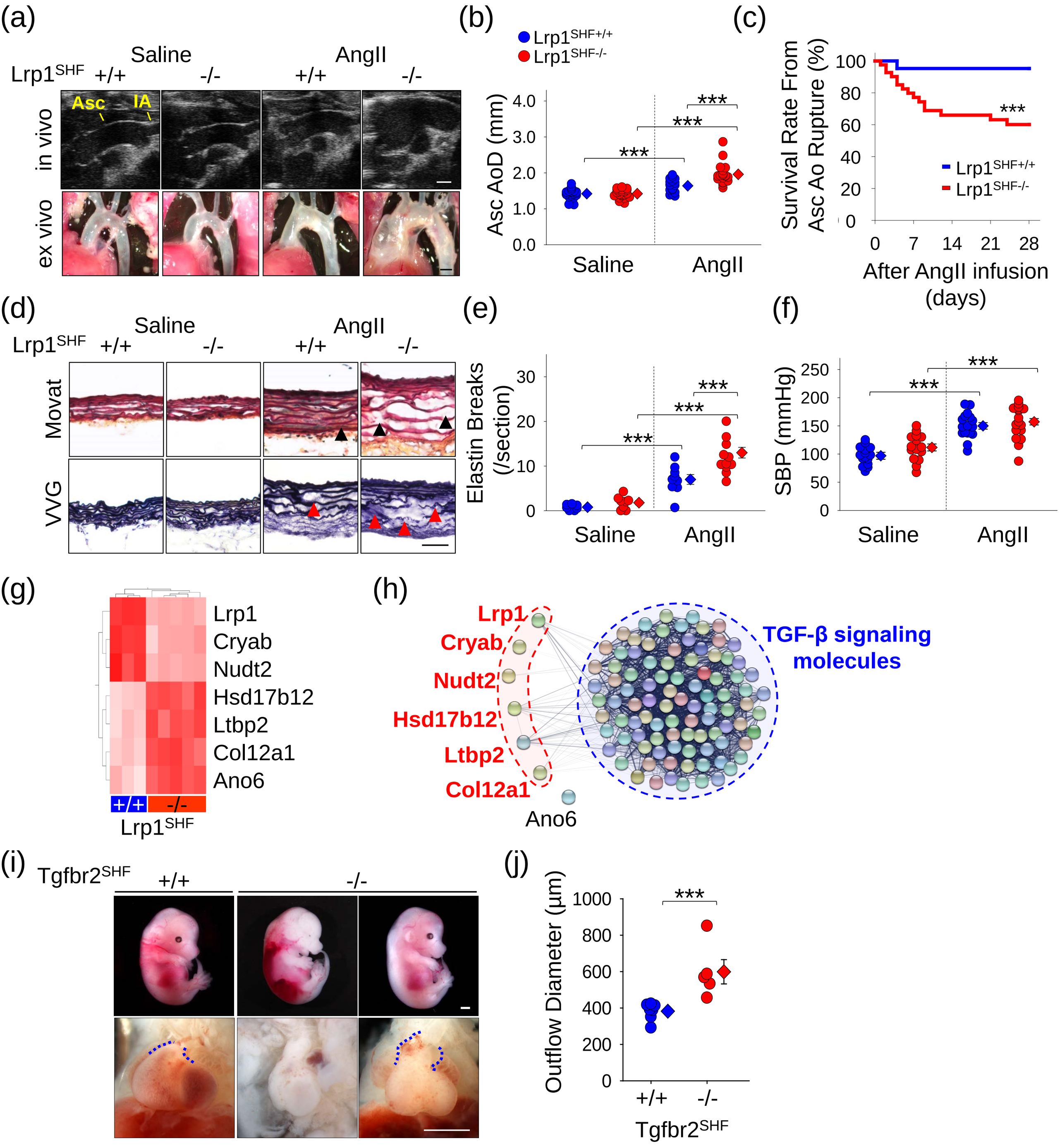
(a)
Saline
AngII
Lrp1SHF +/+ -/- +/+ -/-
Asc
IA
in vivo
ex vivo
(b)
Lrp1SHF+/+
Lrp1SHF-/-
Asc AoD (mm)
4.0
3.0
2.0
1.0
0.0
***
***
***
Saline
AngII
(c)
Survival Rate From Asc Ao Rupture (%)
100
80
60
40
20
0
***
Lrp1SHF+/+
Lrp1SHF-/-
0 7 14 21 28
After AngII infusion (days)
(d)
Saline
AngII
Lrp1SHF +/+ -/- +/+ -/-
Movat
VVG
(e)
Elastin Breaks (/section)
30
20
10
0
***
***
***
Saline
AngII
(f)
SBP (mmHg)
250
200
150
100
50
0
***
***
Saline
AngII
(g)
Lrp1
Cryab
Nudt2
Hsd17b12
Ltbp2
Col12a1
Ano6
+/+ -/-
Lrp1SHF
(h)
Lrp1
Cryab
Nudt2
Hsd17b12
Ltbp2
Col12a1
Ano6
TGF-β signaling molecules
(i)
Tgfbr2SHF
+/+ -/-
(j)
Outflow Diameter (μm)
1000
800
600
400
200
0
***
+/+ -/-
Tgfbr2SHF

Methods

Mice:

The following mice were purchased from The Jackson Laboratory **(Table I)**: ROSA26R^{LacZ} (#003474), *Lrp1* floxed (#012604), *Tgfbr2* floxed (#012603), Wnt1-*Cre* [#022501 (C57BL/6J background, also known as B6-Wnt1-*Cre*2), #022137 (Wnt1-*Cre*2 on a 129S4 background)]. Mef2c-*Cre* mice (#030262) were purchased from the Mutant Mouse Resource and Research Center. For cell tracking studies of the cardiac neural crest (CNC) and second heart field (SHF), either Wnt1-*Cre* (#022501) or Mef2c-*Cre* male mice were bred to ROSA26R^{LacZ} female mice, respectively. To delete *Lrp1* in CNC-derived cells, Wnt1-*Cre* mice were bred with Lrp1 flox female mice. Embryonic lethality, a phenotype of *Lrp1* deletion in CNC-derived cells, was confirmed using 129S4 background Wnt1-Cre strain. Embryos with CNC-specific *Lrp1*-deletion were harvested from *Lrp1* floxed female mice bred with Wnt1-*Cre* (#22137) males. To delete *Lrp1* in SHF-derived cells, Mef2c-*Cre* male mice were crossbred to *Lrp1* floxed female. Wnt1-*Cre* and Mef2c-*Cre* male mice were used for lineage-specific deletion of *Tgfbr2* in CNC and SHF-derived cells, respectively. Because of low incidence of AngII-induced TAA in female mice, only male mice were studied.[1] Mice were housed in ventilated cages with negative air pressure (Allentown Inc). Mouse housing condition is described in **Table II**. Briefly, aspen hardwood chips were used as bedding (#7090A, Harlan Teklad Global). Mice were fed a normal laboratory rodent diet (#2918, Harlan Teklad Global) and provided with drinking water from a reverse osmosis system (pH 6.0 - 6.2) ad libitum. Ambient temperature ranged from 68 to 74 °F and humidity was 50 to 60%. The room's light:dark cycle was 14:10 hr. For mice expiring before the end point, necropsy was performed to determine cause of death. Genotypes were confirmed at termination using DNA isolated from tails or brains using Maxwell tail DNA purification kit (#AS1120, Promega) and PCR with primers shown in **Table III**. All procedures were approved by the University of Kentucky's IACUC.

Pump Implantation:

Saline or AngII (1,000 ng/kg/min, H-1705, Bachem) was infused via a subcutaneously implanted osmotic pump (either Alzet model 2001 for 3 days for experiments using aortic tissues prior to overt pathology, or model 2004 for 28 days, Durect, Cupertino, CA) into male mice at 10 - 14 weeks of age, as described previously.[2] Surgical staples were used to close incision sites and were removed at 7 days after the surgery. Post-operative pain was alleviated by application of topical lidocaine cream (4% wt/wt, LMX4, #0496-0882-15, Eloquest Healthcare, Inc).

Embryonic Study:

To investigate aortic malformation during the prenatal phase, fetuses were harvested from pregnant females on either E11.5 or E12.5. The morning after detection of a vaginal plug in mated females was defined as E0.5 of gestation. Female breeders were euthanized using 300 µl of ketamine/xylazine cocktail (90 mg/kg, 10 mg/kg, respectively), and saline (8 ml) was perfused into the left ventricle. The abdominal cavity of female breeders was subsequently opened and fetuses were dissected free. Gross appearance of fetuses were recorded using a dissection microscope with a high resolution camera (#SMZ800, #DS-Ri1, Nikon) and cranial tissue was retrieved for

genotyping. The embryo's body was immersed in buffered formalin (10% wt/vol). Twenty four hours later, chest wall, pericardium, and atriums were removed gently, and gross appearance of the outflow tract was imaged using a dissection microscope coupled to a high resolution camera. Diameter of the outflow tract was measured at 300 – 400 μm distal of the root in fetuses that survived at the termination.

Aortic Tissue Processing:

Aortic tissue was harvested at either 3 days of infusion for proteomics analysis or at 4 weeks of infusion for other experiments. Mice were euthanized using 300 μl of the ketamine/xylazine cocktail. The thoracic cavity was cut open and saline (8 ml) was perfused through the left ventricle. The following organs and tissues were gently removed: adipose, adrenal gland, bladder, bone, brain, esophagus, kidney, intestine, liver, lung, muscle, pancreas, skin, superior mesenteric artery, spleen, stomach, testis, thymus, and trachea. For gross specimen photography, a black thin plastic sheet was placed beneath the heart and ascending aorta in situ. Then, hearts and thoracic aortas were dissected free, and immersed either in paraformaldehyde (PFA, 4% wt/vol) for gross tissue histology or placed in a mold of OCT for frozen sectioning. For frozen sectioning, serial cross-sections (10 μm) were collected starting at aortic valves and ending at the innominate artery.

Histological Analyses:

To detect β-galactosidase activity, whole tissues and fresh frozen sections (10 μm) were fixed with PFA for either 1 hour at 4°C or 10 minutes at room temperature, respectively. PFA-fixed tissues were preincubated in buffer containing sodium phosphate (100 mM, pH 7.3), $MgCl_2$ (2 mM), sodium deoxycholate (0.01% wt/vol) and NP40 (0.02% wt/vol). X-gal (1 mg/ml, V394A, Promega), potassium ferricyanide (5 mM), and potassium ferrocyanide (5 mM) were added to buffer and samples were incubated overnight at room temperature. Whole tissues were post-fixed with buffered formalin (10% wt/vol). Tissue sections on slides were rinsed free of X-gal, and incubated with eosin (1% wt/vol) for 2 minutes, and cover slipped using glycerol gelatin (GG1, Sigma-Aldrich). Elastin fibers were visualized by illuminating X-gal stained sections using a FITC channel.

Movat's pentachrome and Verhoeff's iron hematoxylin stains were performed to visualize elastin fibers as previously described.[3] Hematoxylin and eosin stain was performed to examine structure of the outflow tract in mouse fetuses.

For immunostaining, fresh frozen sections (10 μm) were fixed with acetone for 10 minutes at −20 °C. Then, sections were incubated subsequently with goat serum for 1 hour at 40 °C. Lrp1 antibody (0.5 μg/ml, #92544, Abcam, **Table IV**) was used as primary antibody. Detection of primary antibodies was visualized with a goat anti rabbit IgG antibody (3 ng/ml, BA-1000, Vector). Isotype matched non-immune rabbit IgG antibody (0.5 μg/ml, I8140, Sigma-Aldrich) was used as negative control. Slides were cover slipped with glycerol gelatin (GG1, Sigma-Aldrich). Images were obtained with a Nikon E600 microscope and analyses were performed using NIS-Elements AR software.

Western Blot Analyses:

Ascending aortic tissue was harvested from mice and endothelial cells were removed using a cotton swab. Aortic tissues were incubated with collagenase type I (#SCR13, Sigma-Aldrich) at 37 °C for 12 minutes. Subsequently, adventitia was gently peeled off using forceps. Aortic tissues were homogenized in cell lysis buffer (#9803, Cell Signaling Technology, Danvers, MA) and protease inhibitor (#P8340, Sigma-Aldrich) using Kimble Kontes disposable Pellet Pestles (#Z359971, DWK Life Science LLC.,). Protein concentrations were measured using DC assay kits (#5000111, Bio-Rad). Equal amounts of protein samples (3 µg) were resolved by SDS-PAGE (10% wt/vol) and transferred electrophoretically to PVDF membranes. After blocking, antibodies against the following proteins were used to probe membranes: Lrp1 (0.4 µg/ml, ab92544, Abcam) and β-actin (1:1000, A5441, Sigma-Aldrich). Then, membranes were incubated with either goat anti-rabbit (1 µg/ml, #PI-1000, Vector Laboratories) or goat anti-mouse secondary antibodies (1:1000, #A2554, Sigma-Aldrich) Immune complexes were visualized by chemiluminescence (#34080, Thermo Scientific) and quantified using a Thermo Scientific myECL Imager.

Ultrasonography:

The ascending aorta was imaged in vivo using a Vevo 2100 ultrasound system with a MicroScan MS550 transducer (40mHz, FUJIFILM VisualSonics Inc) as described previously.[4,5] Briefly, mice were anesthetized using isoflurane (1.0 – 2.5%) and heart rate was adjusted between 400 – 550 beats per minutes during ultrasonography. Aortic luminal diameter was measured at the end diastole in three separate heart beats between the inner edge to inner edge.

Systolic Blood Pressure Measurements:

Systolic blood pressure was measured by a non-invasive tail cuff system (#20269, Kent Scientific) as described previously.[6] Conscious mice were restrained in a holder and put on a heated platform. Blood pressure was measured 20 times at the same time each day for three consecutive days. Data showing < 60 or > 250 mmHg, SD > 30 mmHg, or available cycles < 5 of 20 were excluded.

Mass Spectrometry Assisted Proteomics:

Mouse aortic tissue proteolysis:

Aortic tissues harvested after 3 days of either saline or AngII infusion were minced before submersion in RIPA buffer (#9806, Cell Signaling Technology) supplemented with protease inhibitor cocktail (#P8340, Sigma-Aldrich). Tissue pieces were placed in a Precellys CK14 homogenizing tube with RIPA buffer and ceramic beads (1.4 mm; Bertin Instruments). Samples were homogenized on a Precellys 24 tissue homogenizer using three 10 second cycles at 5,000 rpm. Debris were removed by centrifugation for 10 minutes at 4 °C and protein concentrations of supernatant samples were measured using the Pierce BCA Protein Assay (#23225, Thermo Fisher). Equal amounts of protein (10 µg) for each aortic segment were processed using the PreOmics iST in solution trypsinization kit (#00027, PreOmics) according to manufacturer's recommended protocols. The final peptide precipitate was dissolved in

sample buffer (40 µl, 5% acetonitrile, 0.5% formic acid in mass spectrometry grade water).

Mass spectrometry (MS):

Data-dependent acquisition (DDA, unbiased peptide sampling) - the peptides were diluted [1/2] and analyzed using the Orbitrap Fusion Lumos Tribrid mass spectrometer (Thermo Fisher Scientific) fronted with an Easy-Spray ion source, and coupled to an Easy-nLC1000 HPLC pump (Thermo Fisher Scientific). The peptides were separated using a dual column set-up: an Acclaim PepMap RSLC C18 trap column, 75 µm × 20 mm; and an EASY-Spray LC heated (45 °C) column, 75 µm × 250 mm (Thermo Fisher Scientific). An aqueous to organic gradient (solvent A, 0.1% formic acid in MS-grade water mixed with solvent B, 0.1% formic acid in MS-grade acetonitrile) was generated with a flow rate of 300 nl/min from 5 to 21% solvent B for 75 minutes, 21 to 30% Solvent B for 15 minutes, followed by ten minutes of a 'jigsaw wash', alternating between 5 and 95% Solvent B. The instrument was set to 120 K resolution, and the top N precursor ions in a 3 second cycle time (within a scan range of 400-1500 m/z; isolation window, 1.6 m/z; ion trap scan rate, normal) were subjected to collision induced dissociation (collision energy 30%) for peptide sequencing (or MS/MS). Dynamic exclusion was enabled (60 seconds).

MS/MS data analysis:

The MS/MS data were queried against the mouse UniProt database (downloaded on August 1, 2014) using the SEQUEST search algorithm, via the Proteome Discoverer (PD) Package (version 2.2, Thermo Fisher Scientific), using a 10 ppm tolerance window in the MS1 search space, and a 0.6 Da fragment tolerance window for CID. N-terminal acetylation and methionine oxidation were set as a variable modifications, and carbamidomethylation of cysteine residues was set as a fixed modification. In order to quantify peptide precursors detected in the MS1 but not sequenced from sample to sample, we enabled the 'Feature Mapper' node. Chromatographic alignment was done with a maximum retention time (RT) shift of 10 minutes and a mass tolerance of 10 ppm. Feature linking and mapping settings were, RT tolerance minimum of 0 minutes, mass tolerance of 10 ppm and signal-to-noise minimum of five. Precursor peptide abundances were based on their chromatographic intensities and total peptide amount was used for normalization. Peptides assigned to a given protein group, and not present in any other protein group, were considered as unique. Consequently, each protein group is represented by a single master protein (PD Grouping feature). We used unique and razor peptides per protein for quantification.

Statistical Analyses:

Statistical analyses were performed using SigmaPlot version 14.0 (SYSTAT Software Inc.). Normality and equal variance were assessed prior to comparison by Shapiro-Wilk test and Brown-Forsythe test, respectively. For data comparison between two groups of equivalent variance and normal distribution, two-sided Student's t-test was performed. To compare multiple groups that passed normality and equal variance tests, two Way ANOVA with Holm-Sidak test was used. Kruskal-Wallis followed by

Dunn's test was used for data that failed normality or equal variance test. $P < 0.05$ was considered statistically significant.

Statistical analyses for proteomics data were performed by Qlucore Omics Explorer 3.5 (Qlucore). For a principal component analysis (PCA) plot and heat maps, proteins were filtered by their q-value of two-group or multiple group comparisons. The q-value was calculated using Qlucore and $q = 0.1$ was used as a threshold. Protein clustering in the PCA plot was performed by k-means clustering in Qlucore.

Protein-protein interaction networks were constructed by the STRING database.[7] Interactions were acquired using the following thresholds (confidence interaction scores ≥ 150, active interaction sources = text mining, experiments, databases, co-expression, neighborhood, gene fusion, co-occurrence). For the interaction of Lrp1 in Supplemental Figure 1b, the STRING program was launched using detected 42 proteins with Lrp1. For the interaction of Tgfbr2 in Fig 2h, the STRING program was performed using detected 7 proteins and genes related to TGF-β signaling pathway which were cited from the KEGG PATHWAY Database (#04350). Protein interaction figures were modified using Photoshop CC 2019 (Adobe Systems Incorporated).

References

1. Robinet, P.*, et al. Arterioscler Thromb Vasc Biol* **38**, 292-303 (2018).
2. Lu, H.*, et al. J Vis Exp* (2015).
3. Rateri, D.L.*, et al. Am J Pathol* **184**, 2586-2595 (2014).
4. Sawada, H.*, et al. J Vis Exp* (2019).
5. Chen, J.Z.*, et al. Circ Rep* **1**, 199-205 (2019).
6. Daugherty, A., Rateri, D., Hong, L. & Balakrishnan, A. *J Vis Exp* (2009).
7. Szklarczyk, D.*, et al. Nucleic Acids Res* **47**, D607-d613 (2019).

Table I. Mouse Strains

Strain	Company	Stock #
ROSA26R^{LacZ}	The Jackson Laboratory	003474
Lrp1 floxed	The Jackson Laboratory	012604
Tgfbr2 floxed	The Jackson Laboratory	012603
Wnt1-*Cre* (C57BL/6J)	The Jackson Laboratory	022501
Wnt1-*Cre* (129S4)	The Jackson Laboratory	022137
Mef2c-*Cre*	Mutant Mouse Resource and Research Center	030262

Table II. Mouse Housing Conditions

	Mouse Housing Conditions	Note
Set Temperature range	68 - 74 °F (20 - 23 °C)	
Humidity range	50 - 60%	
Light cycle (light:dark)	14:10 hours	
Water	RO Water	ad libitum
Standard feed	18% Protein Rodent Diet, # 2918, Teklad Irradiated Global	ad libitum
Standard bedding	Aspen hardwood chips, #7090A, Harlan Teklad Global	
SPF	Yes	

Table III. Primer Sequences for Genotyping PCR

Gene		Primer Sequence
Cre	Forward	ACCTGAAGATGTTCGCGATT
	Reverse	CGGCATCAACGTTTTCTTTT
IL-2	Forward	CTAGGCCACAGAATTGAAAGATCT
	Reverse	GTAGGTGGAAATTCTAGCATCATCC
Lrp1 Flox	Forward	CATACCCTCTTCAAACCCCTTCCTG
	Reverse	GCAAGCTCTCCTGCTCAGACCTGGA
Lrp1 delta Flox	Forward	AAAGAGGCACTAGAGCGCAG
	Reverse	CCTCTGGCTGCAAAAATGCAC
Tgfbr2 Flox	Forward	TATGGACTGGCTGCTTTTGTATTC
	Reverse	TGGGGATAGAGGTAGAAAGACATA

Table IV. Antibodies

Target antigen	Vendor	Catalog #	Working Concentration
Rabbit Lrp1	Abcam	Ab92544	0.4 μg/ml for Western blot 0.5 μg/ml for Immunostaining
Mouse β-actin	Sigma-Aldrich	A5441	1:1000
Goat anti-rabbit IgG	Vector	PI-1000	1 μg/ml
Goat anti-mouse IgG	Sigma-Aldrich	A2554	1:1000
Non-immune rabbit IgG	Sigma-Aldrich	I8140	0.5 μg/ml

Supplemental Figure 1

(a) E12.5

(b) E11.5

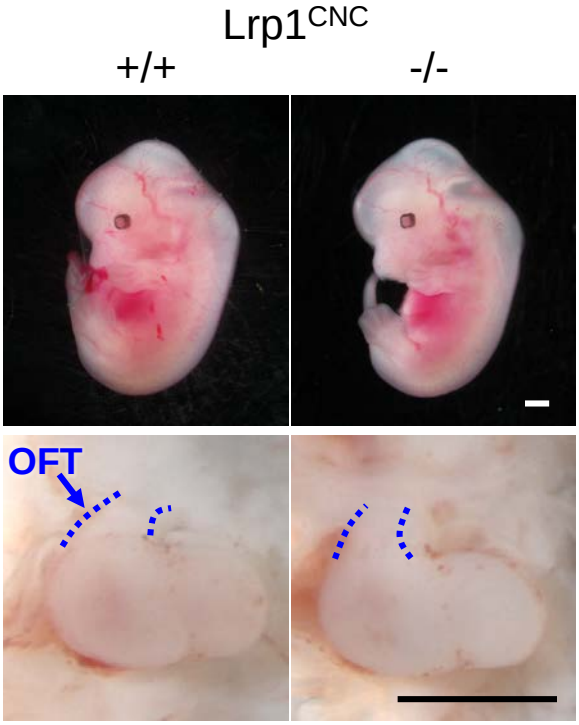

Supplemental Figure 1.
Embryonic lethality of *Lrp1* deletion in CNC-derived cells. **(a)** Gross appearance of wild type and CNC-specific *Lrp1*-deleted fetuses at E12.5. **(b)** Gross appearance of fetuses and outflow tract in wild type and CNC-specific Lrp1-deleted fetuses at E11.5. Scale bar = 1 mm. Blue dotted lines = outflow tract (OFT).

Supplemental Figure 2

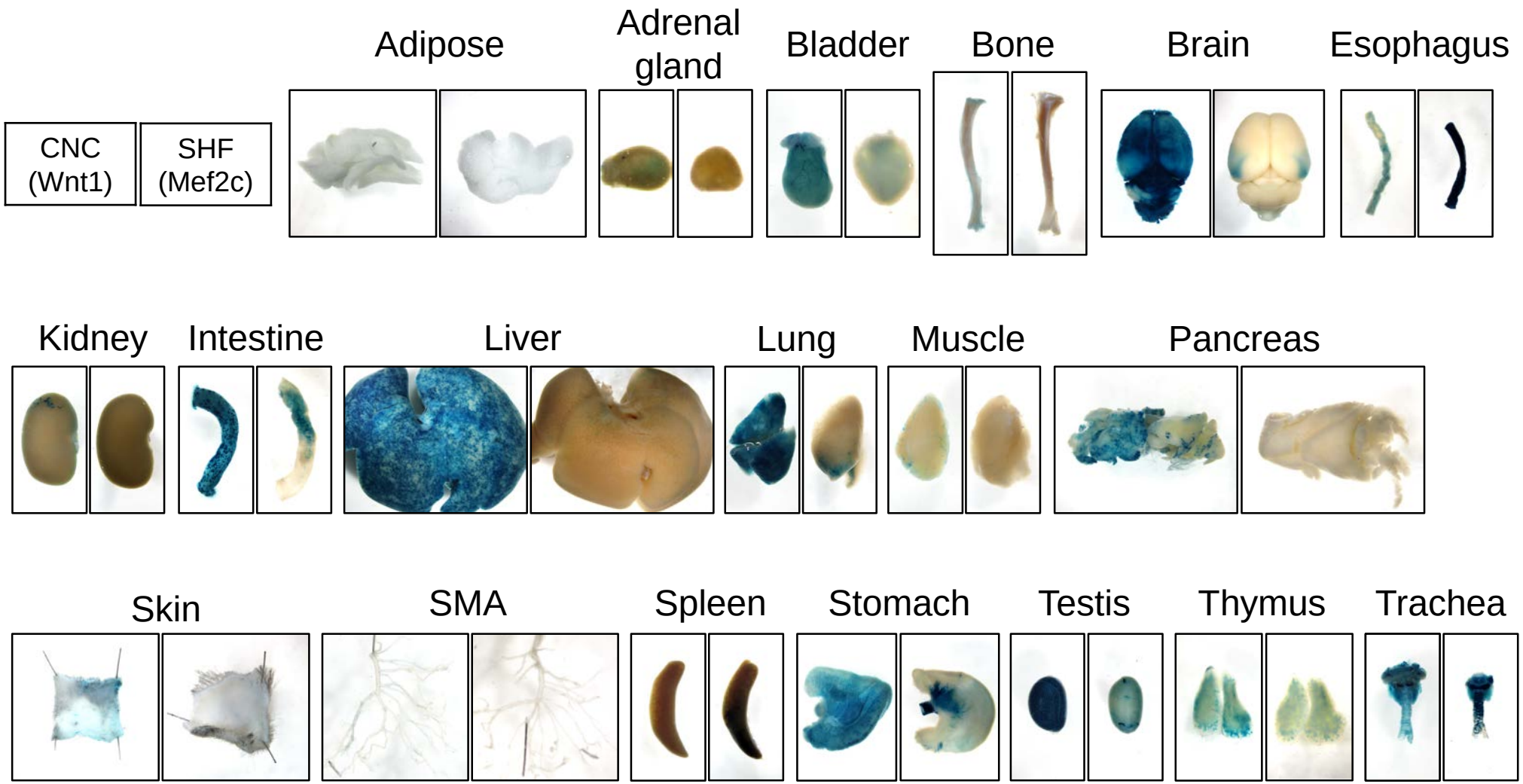

Supplemental Figure 2.
Representative X-gal staining images of major organs from Wnt1- or Mef2c-*Cre* ROSA26R^{LacZ} male mice. CNC = cardiac neural crest, SHF = second heart field, SMA = superior mesenteric artery.

Supplemental Figure 3

(a)

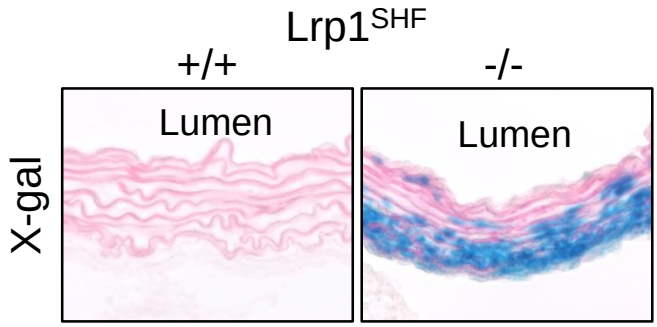

(b)

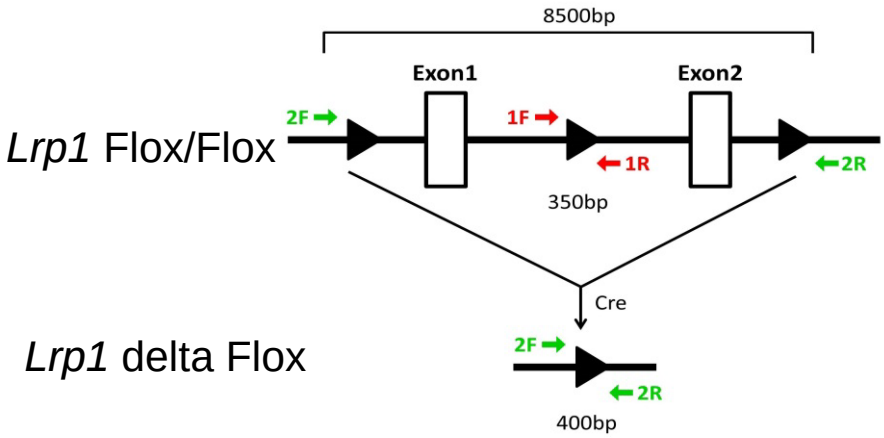

(c) *Cre*

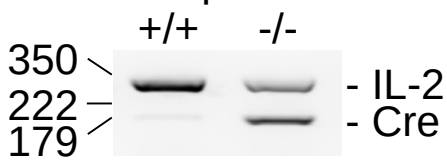

(d) *Lrp1*

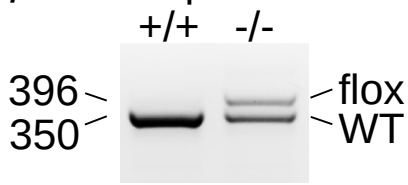

(e)

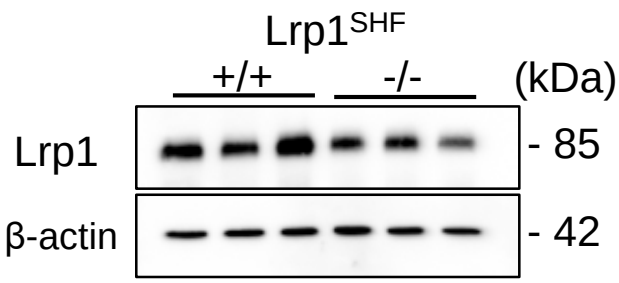

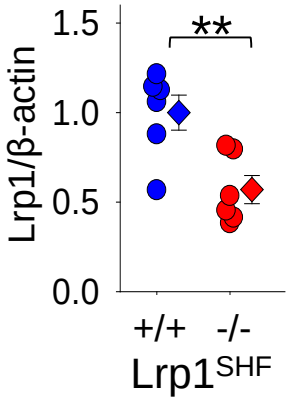

(f)

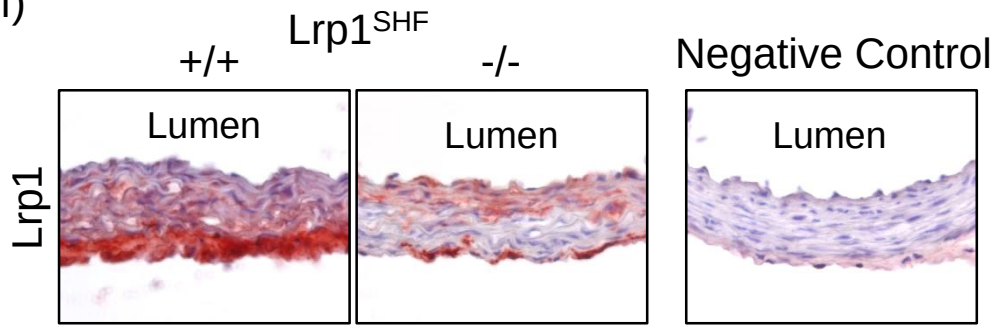

Supplemental Figure 3. Verification of *Lrp1* deletion in SHF-derived cells in Mef2c-*Cre* +/0 Lrp1 floxed mice. Aortic tissues were harvested from SHF-specific *Lrp1*-deleted mice and wild type littermates at 10 - 12 weeks of age (male, n = 3 – 6). **(a)** Representative aortic images of X-gal staining. **(b)** Primer design for PCR of *Lrp1* flox sequence. Red and green primers were used for PCR. Representative PCR results of **(c)** *Cre* and **(d)** *Lrp1* flox sequences. Representative images of **(e)** Western blot for Lrp1 and β-actin and **(f)** immunohistochemistry for Lrp1. As negative control, a section was incubated with non-immune rabbit IgG antibody. ** = $p < 0.01$.

Supplemental Figure 4

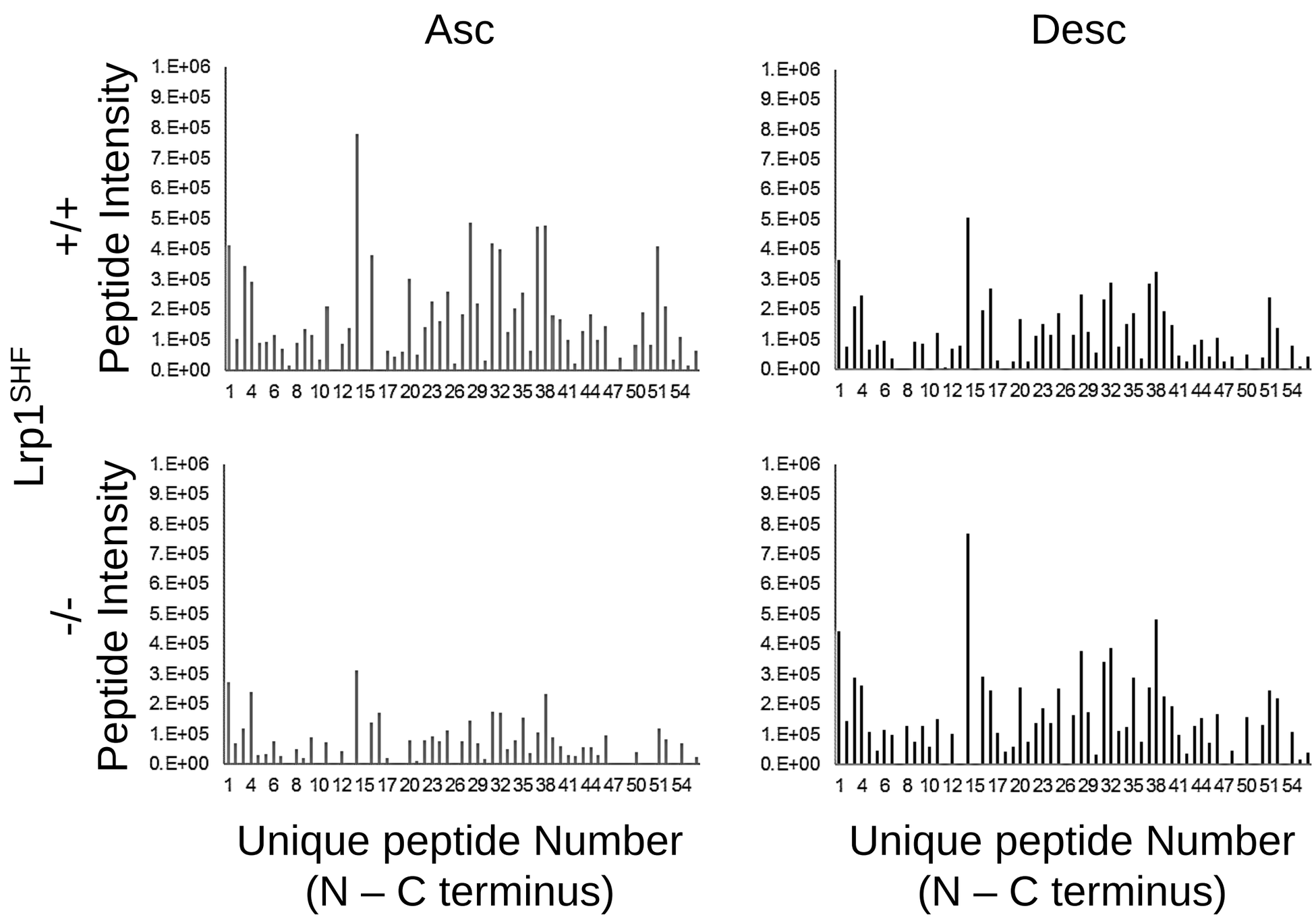

Supplemental Figure 4. Verification of *Lrp1* deletion in SHF-derived cells by proteomics analysis. The normalized peptide intensities of Lrp1 were exported from Proteome Discoverer 2.2. The peptide intensities were plotted from N-to-C-terminus with the numbering conserved across the ascending and descending aortas of SHF-specific Lrp1 deficient mice and wild type littermates.